Planetary and Space Science 61 (2012) 79–84

Contents lists available at ScienceDirect

Planetary and Space Science

journal homepage: www.elsevier.com/locate/pss

Is hydrodynamic escape from Titan possible?

A. Schaufelberger [a,*], P. Wurz [a], H. Lammer [b], Yu.N. Kulikov [c]

[a] Physikalisches Institut, Universität Bern, Sidlerstrasse 5, CH-3012 Bern, Switzerland
[b] Space Research Institute, Austrian Academy of Sciences, Schmiedlstr. 6, A-8042 Graz, Austria
[c] Polar Geophysical Institute, Russian Academy of Sciences, Khalturina 15, 183010 Murmansk, Russian Federation

ARTICLE INFO

Article history:
Received 6 December 2010
Received in revised form
18 March 2011
Accepted 21 March 2011
Available online 1 April 2011

Keywords:
Titan
Exosphere
Hydrodynamic escape

ABSTRACT

When examining thermal atmospheric escape, usually either Jeans escape or hydrodynamic escape is considered. Jeans escape, where particles with velocities higher than the escape velocity can escape a planetary atmosphere, is usually considered, when particles in a collision-free region are examined. Hydrodynamic escape, on the other hand, presumes that the outflowing gas can be considered as a continuous, homogeneous medium where neither light, nor heavy particles can be discriminated from each other. Recently, Strobel (2009) applied a so-called 'slow hydrodynamic escape model', which describes cases intermediate between Jeans escape and hydrodynamic escape, for the nitrogen and methane molecules in Titan's upper atmosphere. This model requires an extended quasi-collisional region above the exobase where efficient energy transfer can presumably occur. In this study, we examine the collision probability of nitrogen and methane molecules with ambient atmospheric particles within Titan's exosphere using a modified Monte Carlo code introduced by Wurz and Lammer (2003), to analyze if the 'slow hydrodynamic escape model' is applicable to Titan's exosphere or not. Our results show that the collision probability of nitrogen and methane within Titan's exosphere decreases quickly with height above the exobase. Also, the probability of a nitrogen or a methane molecule to collide with another heavy molecule is far larger than the probability of a collision with a light particle, since in the region where nitrogen and methane are mainly present, the heavy molecules dominate the light molecules by a factor of 10–100. The results of our particle simulation do not confirm the existence of an extended quasi-collisional region above the exobase, where heavy, slow molecules can gain the escape velocity through collisions with light, fast particles.

© 2011 Elsevier Ltd. All rights reserved.

1. Introduction

Ever since the ion neutral mass spectrometer (INMS) on cassini-huygens has provided us with indications of considerably larger than expected loss rates for heavy species from Titan's atmosphere (De La Haye et al., 2007b; Yelle et al., 2008), different models have tried to explain the reason for these loss rates (Strobel, 2009; Johnson, 2009). Some of these models apply non-thermal escape processes where the energy is deposited directly in the exobase region (Lammer et al., 1998; De La Haye et al., 2007a,b; Shematovich et al., 2003; Michael and Johnson, 2005; Wahlund et al., 2005). Other models treat thermal escape processes, where the energy is deposited well below the exobase and is transferred to higher altitudes through collisions and diffusion of the atmospheric particles (Cui et al., 2008; Strobel, 2008, 2009; Yelle et al., 2008). Especially Strobel (2008, 2009) introduced a hypothesis of so-called 'slow hydrodynamic escape' based on the early pioneering works of Watson et al. (1981) and Kasting and Pollack (1983) who studied hydrodynamic escape of an atomic hydrogen rich thermosphere from a terrestrial planet due to solar EUV heating by applying idealized hydrodynamic equations. From their thermospheric model these authors obtained supersonic flow solutions for which the sonic point was reached at a distance of about 30 planetary radii. These authors argued that supersonic hydrodynamic escape of atomic hydrogen was possible from Earth's atmosphere if it was dominated by hydrogen even if it was exposed to the present time Sun's EUV flux. However, as pointed out by Lammer et al. (2008), these studies assumed that the hydrodynamic fluid equations applied above the exobase level are not internally self-consistent and atom velocities at the exobase level were much lower than the escape velocity. The question remains if the atoms can really achieve their supersonic speed and 'slow hydrodynamic escape' can occur. In the past and current year, several Monte Carlo simulations were conducted to reassess the applicability of the models treating thermal escape processes (Johnson, 2009, 2010; Tucker and Johnson, 2009; Volkov et al., 2011). The findings of these simulations lead to the conclusion that the applied thermal

* Corresponding author. Tel.: +41 31 631 85 46.
E-mail address: schaufelberger@space.unibe.ch (A. Schaufelberger).

0032-0633/$ - see front matter © 2011 Elsevier Ltd. All rights reserved.
doi:10.1016/j.pss.2011.03.011

hydrodynamic escape models are inapplicable to Titan's exosphere. The major problem arises when trying to confirm the needed energy transfer from lighter, faster particles to heavier, slower particles within Titan's exosphere. The aim of this study is to evaluate the collision probabilities of N_2 and CH_4 molecules in Titan's exosphere, since this transfer presumably occurs through thermal conduction. We apply a Monte Carlo code to investigate if the conversion of internal thermal energy of the neutral gas into kinetic energy of the flow is retarded by the lack of collisions above the exobase. If the flow of neutral particles cannot be accelerated anymore, it is not clear that either the sonic or escape velocity can be reached. In Section 2 we describe the applied Monte Carlo model, in Section 3 we present our results and in Sections 4 and 5 we discuss our results.

2. Model

The exobase is usually defined as the level, where the mean free path is equal to the local scale height. Strictly speaking, the exobase is not a line but a region, and its level should be different for each species, due to their different characteristics. In this study we evaluate the distance where collisions can still occur above the exobase level. We initialize 10^6 methane and 10^6 nitrogen molecules and follow each particle separately along its individual trajectory from the exobase up to a height of 20 times the exobase scale height. The exobase height was set equal to 1429 km and the temperature was set to be 149 K (both values are taken from Waite et al., 2005). These values are in good agreement with the exobase height and exobase temperature also calculated from the INMS data by different authors. De La Haye et al. (2007b) calculate the exobase height as being between 1400 and 1450 km and the exobase temperature as being between 149 and 162.3 K, and Cui et al. (2009) calculate a height of ~ 1500 km and a temperature of 151 K.

In our model, we assign to each particle an initial velocity equal to the product of the most probable speed and a Gauss derivative. The most probable speed is given as the maximum value of the velocity probability density function

$$F(v) = 4\pi\left(\frac{m}{2\pi k_B T_{exo}}\right)^{3/2} v^2 \exp\left(-\frac{mv^2}{2k_B T_{exo}}\right), \tag{1}$$

and is equal to

$$v_p = \sqrt{\frac{2k_B T_{exo}}{m}}, \tag{2}$$

where k_B is the Boltzmann constant, T_{exo} is the exobase temperature of the gas, and m is the particle's mass. Each particle's initial velocity is split up into three components (v_x, v_y, v_z) according to the release angles, which are uniformly distributed over 2π (see Wurz and Lammer, 2003; Wurz et al., 2007). The two components perpendicular to the radial component are combined to one vector called the tangential velocity ($v_{tan} = \sqrt{v_x^2 + v_y^2}$) while the third component corresponds to the radial velocity ($v_{rad} = v_z$).

Once a particle has obtained two initial velocity components (tangential and radial velocity), its collision-free keplerian trajectory is calculated. To implement the keplerian trajectories, we applied an eighth order f - and g-series algorithm. Let $\mathbf{r}_0 = \mathbf{r}(t_0)$ and $\mathbf{v}_0 = \mathbf{v}(t_0)$ be the particle's position and velocity vectors at time t_0. Then, $\mathbf{r}(t)$ and $\mathbf{v}(t)$, the position and velocity vectors at time t, can be written as

$$\mathbf{r}(t) = f\mathbf{r}_0 + g\dot{\mathbf{r}}_0, \tag{3}$$

$$\mathbf{v}(t) = \dot{f}\mathbf{r}_0 + \dot{g}\dot{\mathbf{r}}_0, \tag{4}$$

where f and g are the coefficient series, and $\dot{f}$ and $\dot{g}$ are their derivatives with respect to time:

$$f = 1 - \frac{u}{2}(t-t_0)^2 + \frac{uz}{2}(t-t_0)^3 + \cdots, \tag{5}$$

$$g = t - \frac{u}{6}(t-t_0)^3 + \frac{uz}{4}(t-t_0)^4 + \cdots, \tag{6}$$

where $\mu = GM$, $u = \mu r_0^{-3}$, $z = \mathbf{r}_0\dot{\mathbf{r}}_0 r_0^{-2}$ and where G is the gravitational constant and M is Titan's mass.

In our case, where we want to compute the collision probability as a function of height, we do not use constant time steps but constant altitude steps. At each point in our simulation, we take the particle's current velocity and compute the time needed to travel the length of the altitude step. This required time is then used as our next time step. The step size of the simulation is constant at 1 km which is negligible compared to the scale height and mean free path of N_2 and CH_4 at Titan's exobase. At each altitude step, the arc-length traveled and the radial and the tangential velocities are stored.

Having computed all 10^6 methane and 10^6 nitrogen molecules' trajectories, we also used the Monte Carlo model to model H, H_2, HCN and the hydrocarbons present in Titan's exosphere. These particles were not further investigated, but used, together with the methane and nitrogen molecules, to compute the total vertical density profile in Titan's exosphere $n(r)$. Each species' vertical density profile is computed separately by multiplying the species' exobase density with the fraction of particles present at each altitude step. The total vertical density profile is equal to the sum of all species' vertical density profiles. Using this total vertical density profile, we can compute the collision probability of a particle moving upward to collide with the ambient atmospheric molecules along an element of its trajectory starting at the radial distance r_j and ending at the distance r_{j+1}:

$$P_i(r_{j,j+1}) = 1 - e^{-\int_{r_j}^{r_{j+1}} n(r)\sigma_i \, d\mathbf{s}}, \tag{7}$$

where i denotes the species, r_j and r_{j+1} are the positions of the particle at the beginning and the end of the altitude step, respectively, $n(r)$ is the height dependent total atmospheric density, σ_i is the particle's cross-section and $d\mathbf{s}$ is the line segment along the particle's path. We set σ_i equal to 3.91×10^{-15} cm^2 for N_2 and 4.75×10^{-15} cm^2 for CH_4 (Chernyi and Losev, 2007).

As we mentioned, the step size is small compared to the particle's mean free path, thus we can assume $n(r)$ to be constant within one altitude step. The probability of a particle within the altitude step $[j,j+1]$ to experience a collision can therefore be simplified to

$$P_i(r_{j,j+1}) = 1 - e^{-n(r_j)\sigma_i \Delta s_j}, \tag{8}$$

where $n(r_j)$ is the atmospheric density at r_j, and Δs_j is the average distance traveled (arc-length) within the given altitude range.

We also compute the total probability for an upward moving particle to collide along its way from its current position in the exosphere r to the upper boundary of our model r_{UB}, above which we assume no collisions. For this we calculate first the total number of collisions along the particle trajectory, that is along its path over the altitude interval $[r_j, r_N]$, which is given by the integral

$$N_{i_{col}}(r) = \int_r^{r_{ub}} n(r')\sigma_i \, ds', \tag{9}$$

where $n(r')$ is the altitude dependent total density of the atmosphere, σ_i is the particle's cross-section and ds' is the arc-length corresponding to the infinitesimal height change dr'. Substituting integration with discrete summation, we get for calculation of the total number of collisions that the particle undergoes on its way from r_j to $r_N(=r_{UB})$ the following equation:

$$N_{i_{col}}(r_j)=\sum_{k=j}^{N-1} n(r_k)\sigma_i \Delta s_{[k,k+1]}, \quad (10)$$

where $n(r_k)$ is the average total density and $s_{[k,k+1]}$ is the arc-length in the interval $[r_k, r_{k+1}]$. The total collision probability can then be calculated as

$$P_{i_{tot}}(r_j)=1-e^{-N_{i_{col}}(r_j)}, \quad (11)$$

where $N_{i_{col}}(r_j)$ is the total number of collisions the particle suffers along its way from r_j to the upper boundary of the modeling region.

3. Results

We present the radial velocity, the tangential velocity and the density distributions for 1,000,000 nitrogen and 1,000,000 methane particles in Titan's exosphere. The atmospheric constituents considered when computing the total vertical density profile are H, H_2, N_2, CH_4, HCN, C_2H_2, C_2H_4, C_2H_6 and C_4H_2. We only show profiles up to a height of 1000 km above the exobase, since this is the region where in the model of Strobel (2009) collisions are assumed to occur and to provide thermal conduction.

3.1. Velocities

Fig. 1 shows the mean radial velocity, the mean tangential velocity and the particle density of the N_2 and the CH_4 components in Titan's exosphere as a function of height above the exobase. Also depicted, for comparison, is the theoretical escape velocity as a function of height. According to our results, no N_2 molecule and no CH_4 molecule in the exosphere is fast enough to escape Titan's gravity. The molecules' mean velocity is well below the escape velocity at all heights in the exosphere, thus Jeans escape is expected to be negligible.

3.2. Densities

Fig. 2 presents the density profiles of the H, H_2, N_2 and CH_4 constituents in Titan's exosphere. The values for each species' density curve were calculated using our Monte Carlo model. Since we do not include any collisions when modeling our particles' ballistic trajectories, there is a risk of our density profiles dropping off too quickly close to the exobase. We therefore initialized our density profiles in such a way, that our N_2, CH_4 and H_2 values match the INMS density profiles presented by Waite et al. (2005) and Cui et al. (2008) at one scale height above the exobase. To create these profiles, we used a step size of 1 km for the 10^6 N_2 and CH_4 molecules we modeled, and a step size of 10 km for the 10^5 H and H_2 particles we modeled. Also shown, for comparison, are the density profiles measured by INMS. Below ~1759 km (i.e., 330 km above the exobase), the exosphere consists mainly of N_2 and CH_4. At about 1759 km, the heavy molecules start to vanish while H_2 and H start to dominate. Also notable is that while the N_2 molecules dominate over the CH_4 molecules close to the exobase level, the CH_4 molecules start to dominate over N_2 at about 500 km above the exobase level.

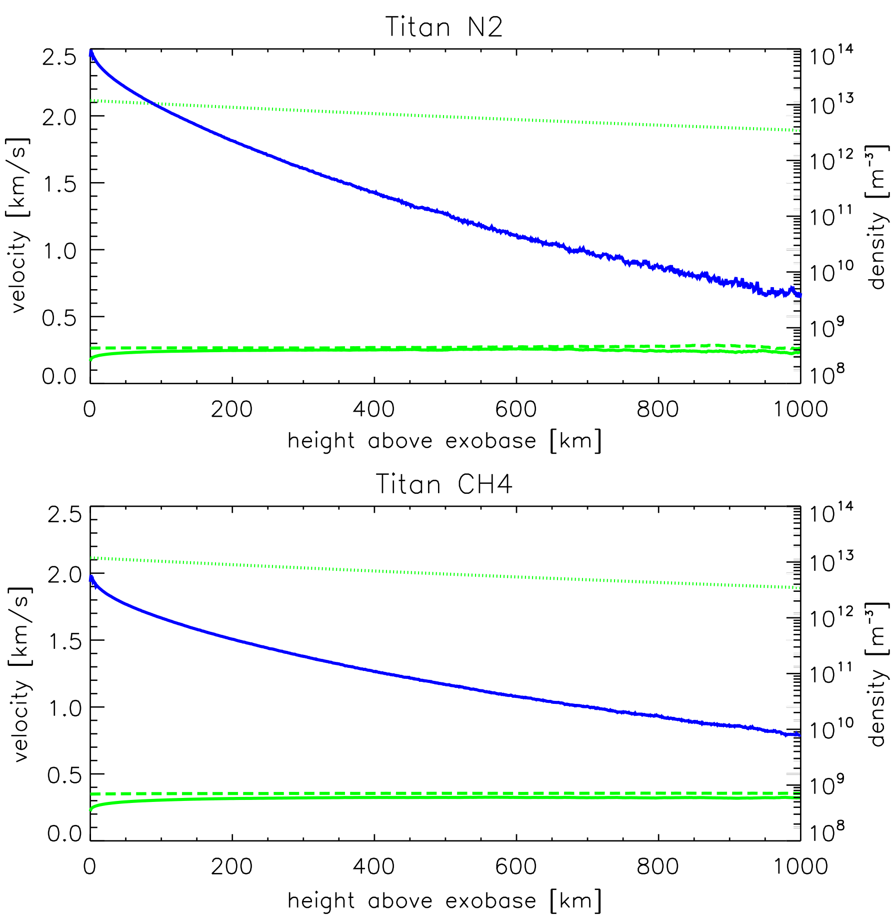

Fig. 1. Velocity and density profiles for the N_2 (top) and CH_4 (bottom) component in Titan's exosphere as a function of height above the exobase. The plot shows $V_{tangential}$ (long dashed green line) and V_{radial} (solid green line) as well as the particle density (solid blue line). Also depicted is the escape velocity (dotted green line).

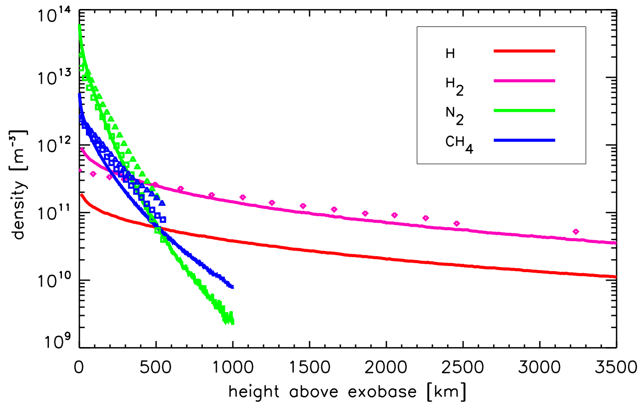

Fig. 2. Densities of the H (red), H_2 (pink), N_2 (green) and CH_4 (blue) component in Titan's exosphere. Also shown are the density profiles measured by INMS. The data points for N_2 and CH_4 were taken from Figure 7 in De La Haye et al. (2007b) (triangle = TA ingress flyby, square = T5 ingress flyby) whereas the data points for H_2 were taken from Figure 1 in Cui et al. (2008) (diamond = average of 14 inbound flybys).

3.3. Collision probabilities

Fig. 3 depicts the volume mixing ratios, the collision probabilities per altitude step and the total collision probabilities as a function of height above the exobase. Also shown is the level, where the light, fast molecules start to dominate over the heavy, slow molecules. The plot shows that the collision probability per altitude step drops below 0.1 percent at $\sim$400 km above the exobase. Table 1 lists the collision probability and the total collision probability at the exobase, at 100 km, at 330 km and at 1000 km above the exobase. The total number of collisions along the particle trajectory starting at the exobase is 0.43 for an N_2 molecule with a radius of 3.53 Å and 0.56 for a CH_4 molecule with a radius of 3.89 Å, respectively.

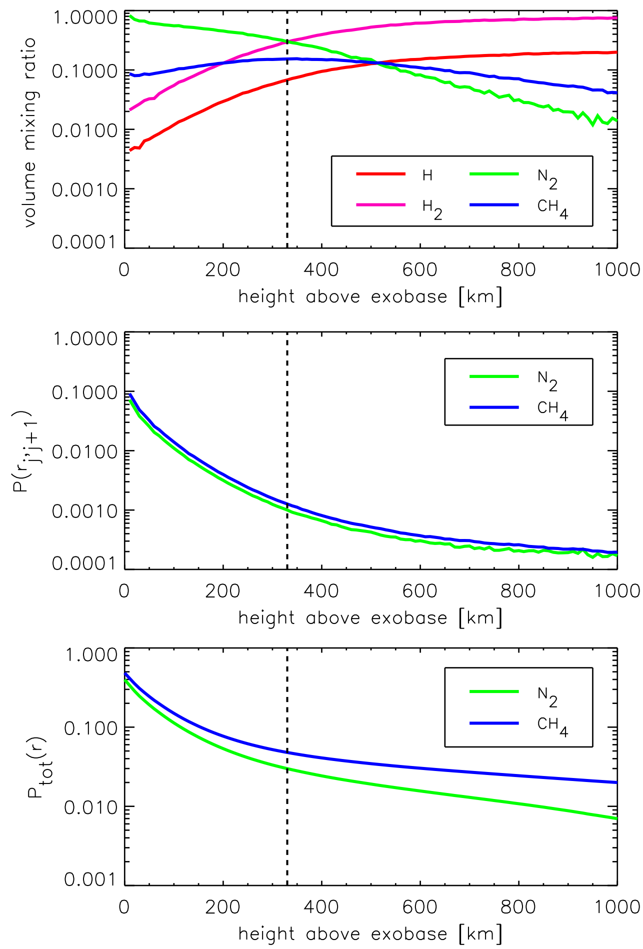

Fig. 3. Volume mixing ratios (top) for the H (red), H_2 (pink), N_2 (green) and CH_4 (blue) components, collision probabilities per altitude step (middle) for the N_2 (green) and CH_4 (blue) components and total collision probabilities (bottom) for the N_2 (green) and CH_4 (blue) components in Titan's exosphere. The black dashed line indicates the altitude, where the light particles (H and H_2) start to dominate the heavy particles (N_2 and CH_4).

4. Discussion

4.1. Velocities

We first compare our computed total exobase velocity to theoretical values to determine the performance of the initialization in our model. For both species (N_2 and CH_4), we compare the mean total velocity at the exobase to the Maxwellian mean magnitude of the velocity vector ($\overline{v}_{tot,max} = \sqrt{8k_BT/\pi m}$). The exobase velocities for N_2 and CH_4 computed from our simulations are 335.87 and 443.48 ms^{-1} and agree well with the theoretical values of 335.94 and 443.70 ms^{-1}. Note that in Fig. 1 the mean radial velocity of both species increases with altitude. This is an effect of gravitational filtering, due to which above each altitude step the slowest particles are lost from the population. When computing the thermal energy profile, where the particle densities and their velocities are taken into account, the expected decrease of the kinetic energy with altitude is discernible. We cannot discern an enhancement in the tail of the calculated velocity distribution, i.e., the distribution does not diverge from the Maxwellian above the exobase, which is in agreement with the results obtained by Tucker and Johnson (2009). Above $\sim$600 km from the exobase, the velocity profiles of N_2 start to become wiggly not because the statistics have not converged, but because there are too few particles to provide a well determined average.

Table 1
Collision probabilities and total collision probabilities for a N_2 molecule (cross-section: 3.91×10^{-15} cm^2) and a CH_4 molecule (cross-section 4.75×10^{-15} cm^2) in Titan's exosphere.

		N_2	CH_4
$P(r_{j,j+1})$	Exobase	7.17e−02	9.45e−02
$P(r_{j,j+1})$	100 km above exobase	1.10e−02	1.39e−02
$P(r_{j,j+1})$	330 km above exobase	1.00e−03	1.27e−03
$P(r_{j,j+1})$	1000 km above exobase	1.71e−04	1.96e−04
$P_{tot}(r)$	Exobase	0.399	0.484
$P_{tot}(r)$	100 km above exobase	0.113	0.150
$P_{tot}(r)$	330 km above exobase	0.030	0.048
$P_{tot}(r)$	1000 km above exobase	0.007	0.020

4.2. Densities

We next look at the density profiles in Fig. 2. As mentioned in Section 3, the heavy molecules dominate below $\sim$1759 km (i.e., 330 km above the exobase) whereas at higher altitudes, the lighter, faster particles become the main constituents of the atmosphere. Since the gravitational force acts stronger on heavier particles, the density profiles of the N_2 and the CH_4 molecules drop off very quickly, while the density profiles of the light particles decrease much slower. Our density profiles agree reasonably well with the INMS density profiles, and at the altitude where the light particles start to dominate the heavy particles our density profile is almost identical with the INMS profiles.

4.3. Collision probabilities

As already pointed out in Section 3, most collisions occur close to the exobase, in the region, where the N_2 and CH_4 densities are higher than the H_2 and H densities. At higher altitudes, where fast particles start to dominate, the collision probability per altitude step drops below 0.1 percent. On average, 0.37 and 0.44 out of the total number of collisions (0.40 and 0.48) occur below 1759 km, i.e., more than 92 and 90 percent of collisions occur within this region. Only 0.030 and 0.048 collisions are expected to occur in the region where the lighter, faster particles dominate. The collisions of N_2 and CH_4 with lighter, faster particles within Titan's exosphere are therefore very unlikely to occur.

4.4. Collisions needed for energisation of heavy molecules

We used a separate Monte Carlo simulation to determine a lower boundary on how many collisions are required on average for a N_2 and a CH_4 molecule to be able to reach the escape velocity. In this simulation, we did not determine the trajectories of the particles, but only computed the energy transferred during collisions. We set the initial velocity of the N_2 and CH_4 molecules to their theoretical thermal velocities. As collision partners we considered only hydrogen atoms, which are faster than the molecules under consideration. Since we wanted to estimate a lower boundary on the number of needed collisions, we assumed the collisions to occur in radial direction, i.e., the molecule under consideration receives the maximal possible energy from the hydrogen atom it collides with. The initial hydrogen velocity distribution was set equal to the hydrogen exobase velocity distribution computed by our model. From this distribution, we randomly chose collision partners, calculated the energy that would be transferred to the N_2 or CH_4 molecule under consideration, and added that energy to the molecule's current energy. This process was repeated until the molecule reached escape velocity. Our simulations show that on average at least 44 and 26 collisions, respectively, with faster, outward moving hydrogen atoms are needed for the N_2 and a CH_4 molecules to be accelerated to the escape velocity by the collisional energy transfer, which is equivalent to thermal conduction in the models of Strobel (2008, 2009). These two values are larger by about a factor of 1000 than the average numbers of collisions that are experienced by an N_2 and a CH_4 molecule in the altitude range above 330 km above the exobase where the lighter, faster particles dominate, and this estimate is a lower bound on the number of needed collisions.

5. Conclusion

Several recently published papers have modeled the escape of N_2 and CH_4 as occurring in a regime intermediate between the Jeans escape and hydrodynamic escape. This escape mechanism requires an extended region above Titan's exobase where frequent collisions still occur, where energy can be transferred through collisions from lighter and faster to heavier but slower particles.

We used a Monte Carlo model to calculate the N_2 and the CH_4 molecules on their keplerian trajectories in Titan's exosphere. At each fixed altitude step, we computed the average density, the average radial and tangential velocities and the average line segment along the particles' paths. Comparison with INMS density profiles shows that our density profiles agree sufficiently well with the measured data. Using the average densities, velocities and arc-lengths computed by our model, we calculate the collision probability for an N_2 and a CH_4 molecule with ambient particles within Titan's exosphere.

Our results show that most collisions occur within the first $\sim$400 km above Titan's exobase with N_2 and CH_4 as collision partners. Above $\sim$400 km, where a collision partner is more likely to be H_2 or H, the collision probabilities are very small. This change in dominance of light over heavy particles to heavy over light particles is also discernible at almost an identical height in the INMS data. The computed number of collisions, which would be needed to accelerate an N_2 or a CH_4 molecule to the escape velocity, exceeds the expected number of collisions within Titan's exosphere by more than an order of magnitude, and even much more when only considering the collisions occurring with lighter, faster exospheric species. The discrepancy between the needed number of collisions and the actual number of collisions is so great, that even if we did underestimate the density profiles for H and CH_4, the conclusion that the numbers differ by more than an order of magnitude still holds.

Our results are in agreement with Tucker and Johnson (2009) and do not confirm the escape rates predicted by the 'slow hydrodynamic escape model'. Whereas Tucker and Johnson (2009) include collisions in their model and show that thermal conduction cannot cause a significant enhancement in the tail of the speed distribution, we show that, due to the rapid decrease in collision probability with altitude, collisions between slower and faster particles do not even occur. Our failure to detect any significant tail enhancement in the speed distribution function also shows that there is no evidence that thermal conduction can produce in the exosphere more energetic particles which are able to escape, as suggested by Strobel (2008). We therefore do not agree that the escape is occurring in a regime intermediate between the Jeans escape and hydrodynamic escape and suggest that the so-called 'slow hydrodynamic escape model' is energetically not possible on present Titan. However, one should note that these conclusions for present day Titan should be taken with care for early times, because Titan's upper atmosphere was not likely to remain hydrostatic during the time when the Sun's EUV flux was much higher in the past. As pointed out by Kasting and Pollack (1983), Tian et al. (2008) and Lammer et al. (2008), under such conditions upper atmospheres might remain collisional out to much farther distances than they are at present.

Acknowledgments

A. Schaufelberger and P. Wurz gratefully acknowledge the financial support by the Swiss National Science Foundation.

Yu.N. Kulikov and H. Lammer acknowledge the support by the Helmholtz Association through the research alliance "Planetary Evolution and Life" and through the joined Russian-Austrian project under the RFBR grant P09-02-91002-ANF-a and the FWF grant I199-N16.

References

Chernyi, G.G., Losev, S.A., 2007. Physico-Chemical Processes in Gas Dynamics, vol. 1. Science World, Moscow, Russian Federation.
Cui, J., Yelle, R.V., Volk, K., 2008. Distribution and escape of molecular hydrogen in Titan's thermosphere and exosphere. Journal of Geophysical Research 113.
Cui, J., Yelle, R.V., Vuitton, V., Waite Jr., J.H., Kasprzak, W.T., Gell, D.A., Niemann, H.B., Müller-Wodarg, I.C.F., Borggren, N., Fletcher, G.G., Patrick, E.L., Raaen, E., Magee, B.A., 2009. Analysis of titans neutral upper atmosphere from cassini ion neutral mass spectrometer measurements. Icarus 200, 581–615.

De La Haye, V., Waite Jr., J.H., Cravens, T.E., Nagy, E.F., Johnson, R.E., Lebonnois, S., Robertson, I.P., 2007a. Titan's corona: the contribution of exothermic chemistry. Icarus 191, 236–250.

De La Haye, V., Waite Jr., J.H., Johnson, R.E., Yelle, R.V., Cravens, T.E., Luhmann, J.G., Kasprzak, W.T., Gell, D.A., Magee, B., Leblanc, F., Michael, M., Jurac, S., Robertson, I.P., 2007b. Cassini ion and neutral mass spectrometer data in Titans upper atmosphere and exosphere: observation of a suprathermal corona. Journal of Geophysical Research 112.

Johnson, R.E., 2009. Sputtering and heating of Titan's upper atmosphere. Philosophical Transactions of the Royal Society 367, 753–771.

Johnson, R.E., 2010. Thermally driven atmospheric escape. The Astrophysical Journal 716, 1573–1578.

Kasting, J.F., Pollack, J.B., 1983. Loss of water from venus. I. Hydrodynamic escape of hydrogen. Icarus 53, 479–508.

Lammer, H., Kasting, J.F., Chassefière, E., Johnson, R.E., Kulikov, Y.N., Tian, F., 2008. Atmospheric escape and evolution of terrestrial planets and satellites. Space Science Reviews 139, 399–436.

Lammer, H., Stumptner, W., Bauer, S.J., 1998. Dynamic escape of H from Titan as consequence of sputtering induced heating. Planetary and Space Science 46, 1207–1213.

Michael, M., Johnson, R.E., 2005. Energy deposition of pickup ions and heating of Titan's atmosphere. Planetary and Space Science 53, 1510–1514.

Shematovich, V.I., Johnson, R.E., Michael, M., Luhmann, J.G., 2003. Nitrogen loss from Titan. Journal of Geophysical Research 108.

Strobel, D.F., 2008. Titan's hydrodynamically escaping atmosphere. Icarus 193, 588–594.

Strobel, D.F., 2009. Titan's hydrodynamically escaping atmosphere: escape rates and the structure of the exobase region. Icarus 202, 632–641.

Tian, F., Kasting, J.F., Liu, H., Roble, R.G., 2008. Hydrodynamic planetary thermosphere model: 1. The response of the earths thermosphere to extreme solar EUV conditions and the significance of adiabatic cooling. Journal of Geophysical Research 113, 1111.

Tucker, O.J., Johnson, R.E., 2009. Thermally driven atmospheric escape: Monte Carlo simulations for Titan's atmosphere. Planetary and Space Science 57, 1889–1894.

Volkov, A.N., Johnson, R.E., Orenthal, J.T., Erwin, J.T., 2011. Thermally-driven atmospheric escape: transition from hydrodynamic to Jeans escape. Astrophysical Journal Letters 729 (2), L24 doi:10.1088/2041-8205/729/2/L24.

Wahlund, J.E., Boström, R., Gustafsson, G., Gurnett, D.A., Kurth, W.S., Pedersen, A., Averkamp, T.F., Hospodarsky, G.B., Persoon, A.M., Canu, P., Neubauer, F.M., Dougherty, M.K., Eriksson, A.I., Morooka, M.W., Gill, R., André, M., Eliasson, L., Müller-Wodarg, I.C.F., 2005. Cassini measurements of cold plasma in the ionosphere of Titan. Science 308, 986–989.

Waite, J.H., Niemann, H., Yelle, R.V., Kasprzak, W.T., Cravens, T.E., Luhmann, J.G., McNutt, R.L., Ip, W.H., Gell, D., De La Haye, V., Müller-Wordag, I.C.F., Magee, B., Borggren, N., Ledvina, S., Fletcher, G., Walter, E., Miller, R., Scherer, S., Thorpe, R., Xu, J., Block, B., Arnett, K., 2005. Ion neutral mass spectrometer results from the first flyby of Titan. Science 308, 982–986.

Watson, A.J., Donahue, T.M., Walker, J.C.G., 1981. The dynamics of a rapidly escaping atmosphere: applications to the evolution of Earth and Venus. Icarus 48, 150–166.

Wurz, P., Lammer, H., 2003. Monte-Carlo simulation of Mercury's exosphere. Icarus 164, 1–13.

Wurz, P., Rohner, U., Whitby, J.A., Kolb, C., Lammer, H., Dobnikar, P., Martín-Fernández, J.A., 2007. The lunar exosphere: the sputtering contribution. Icarus 191, 486–496.

Yelle, R.V., Cui, J., Müller-Wordag, I.C.F., 2008. Methane escape from Titan's atmosphere. Journal of Geophysical Research 113.